Computational Investigation of Droplets Behaviour inside Passive Microfluidic Oscillator

Tawfiq Chekifi[1, *], Brahim Dennai[2] and Rachid Khelfaoui[2]

Abstract: Recently, modeling immiscible fluids such as oil and water have been a classical research topic. Droplet-based microfluidics presents a unique platform for mixing, reaction, separation, dispersion of drops and many other functions. In this paper, we suggest a numerical CFD study of microfluidic oscillator with two different lengths of feedback loop. In order to produce simultaneous droplets of gasoil on water, a typical geometry that includes double T-junction is connected to the fluidic oscillator. Droplets production is computed by volume-of-fluid method (VOF). Flow oscillations of droplets were triggered by the Coanda effect of jet flow. The aim of work is to get a high oscillation frequency in the output of this passive device, the influence of hydrodynamics and physics parameters on the droplets frequency in the output of our microsystem is also investigated, the computational results show that, the length of feedback loop, operating pressure and interfacial tension have a significant effect on the droplets dynamic inside microfluidic oscillator. Across the range of low Reynold number, the droplets generation and its dynamics have been accurately controlled by adjusting applying pressure ratio of two phases.

Keywords: Droplet, microfluidics, fluidic oscillator, CFD and VOF (volume of fluid method).

Nomenclature

f: frequency (Hz)	α: phase fraction
R: rayon (mm)	*B:* incline angle of the straight attachment wall
L: length (mm)	σ: the surface tension coefficient
u: velocity (m/s)	τ: time (s)
n: unit vector normal to the interface	CFD: computational fluid dynamics
κ: curvature of the interface	EWOD: Electrowetting on Dielectric
F: the surface tension force	SAW: surface acoustic wave
W: width (mm)	FOLL: fluidic oscillator with long loop

[1]Research Center in Industrial Technologies CRTI, P.O. Box 64, Cheraga Algiers.

[2]University Tahri Mohamed Bechar, ENERGARID LABORATORY, Bechar, Algeria.

*Corresponding Author: Chekifi Tawfiq. E-mail: chekifi.tawfiq@gmail.com

H: depth (mm)   FOSL: fluidic oscillator with short loop

ρ: density (kg/m^3)   HF: height function

μ: dynamic viscosity (kg/m^{-1}·s^{-1})

1 Introduction

Droplets in microfluidic offer many benefits for conducting biochemical [MDS-Ocata (2000); Thiele and Spandl (2008)] medicine [Seto, Tsang, Yung et al. (2003); Jebrail, Bartsch, Patel et al. (2012)], agriculture [Huichun, Gary and Jiaqiang (2012)] and many other research areas. The few decades have seen increasingly rapid advances in the field of droplets based microfluidic, working in this field allows to benefit of reduction in the volume of reagent required, the size of sample required, and the size of devices used for each application. A growing body of literature has investigated droplets manipulation inside Microsystems, such as electro-wetting on dielectric (EWOD) technique [Shah, Ohta, Chiou et al. (2009)], surface acoustic waves (SAW) technique [Renaudin, Tabourier and Zhang (2006)], magnetic manipulation [Yoon, Kim, Lee et al. (2013)], and hydrodynamic techniques [Sarrazin, Bonometti, Prat et al. (2007)], the benefit of the latter is that no part of the device is in moving. One of the most microdevice used for hydrodynamics flow control is microfluidic oscillator [Shakouchi (1989)]. The principle of operation of the oscillator is based on the Coanda effect discovered firstly by Henri Coanda [Davies (1970)], the fluidic oscillators consists in disturbing the flow of jets issuing from a nozzle and expanding between two curved walls will attach to the less curved one or to the wall which is closer from the jet axis [Yang, Chen, Tsai et al. (2007)], which leads it to oscillate and flow into feedback channel. the frequency is a function of the geometry of the actuator, the size and flow provided. One of the first examples of the fluidic oscillators is presented in [Simões, Furlan, Bruzetti et al. (2005)], the authors presented microfluidic oscillator fabricated with SU-8 based epoxy photoresist and conventional photolithography, in this experimental work, authors concluded that the operation of the microfluidic oscillator was a direct function of the length of the feedback loops and of the velocity inside oscillation chamber. In Gregory's study [Gregory, Sullivan, Raman et al. (2007)], it was shown that the external flow field of the microfluidic oscillator is characterised by two operating regimes, separated by a transitional increase in turbulent noise, it is also observed a significant advance in pressure-sensitive paint technology. Bobusch et al.[Bobusch, Woszidlo, Bergada et al. (2013)] have experimentally studied the internal flow characteristics of a fluidic oscillator. Particle image velocimetry (PIV) and time-resolved pressure (TRP) measurements were used in water to visualize and quantify the internal flow patterns. The authors provided detailed results on the oscillation mechanism, the interaction between the main chamber and feedback loops. In addition, a growing recirculation bubble between the main jet and the attachment wall is identified. A recent review of the literature on this topic was reported by James and Gregory [Gregory and Tomac (2013)], the authors investigated the historical development of fluidic oscillators, the different concepts used as fluidic oscillator and their application to flow control. It was concluded a little awareness of the historical development work that has been done. Another research work on this fluidic device was performed by Yanrong et al.

[Yanrong, Someya, Koso et al. (2013)], in this work numerical and experimentation using high time-resolved particle imaging velocimetry were conducted, in order to identify the flow characteristics in the fluidic oscillator working under low-Reynolds-number water flow. The authors shown that the Strouhal number was not constant and the frequency was not linear with respect to the flow rate. Furthermore, the mechanism of the small-scale feedback fluidic oscillator was clarified by considering the time for a jet to oscillate inside the oscillation chamber. More recent evidence [Tesař (2015)] suggested a new fluidic oscillator configuration for High-frequency fluidic oscillator, the author presented a new oscillation principle, with stationary rotating between both attachment walls. Moreover, three distinct regimes were identified by increasing air flow rate has shown. at low Reynolds numbers; Re~2600 to Re~6000, oscillating at fr=1.7 kHz and fr~5 kHz, respectively. Even that higher frequency fr~8.2 kHz was observed with higher Re. In very recent paper by Matthew et al. [Lakebrink, Mani and Winkler (2017)] a numerical simulations of flow through a highly offset S-duct diffuser, with small Mach number, were presented using the Boeing Computational Fluid Dynamics approach, the author observed two primary regimes flow inside the oscillator; the first one is characterized by around 13 kHz with the sweeping jet. Whereas, the second regime had a frequency of around 200 kHz related to the breakdown of the jet. Additionally, A time-accurate Delayed Detached Eddy Simulation (DDES) of the diffuser with fluidic feedback oscillators was investigated and validated against experimental data.

Recent advances in numerical software and codes have made it possible to simulate the effect of active flow control devices on major aircraft components. Computational fluid dynamics (CFD) provides many information on flow details that are difficult to measure experimentally in some complicated devices [Kobayashi, Vladisavljević, Uemura et al. (2011)]. In recent years, different techniques were developed for interface tracking [Yan, Guo and Wen (2012)]. Usually, the interface that separates the immiscible phases can be solved using lattice Boltzmann method (LBM) [Gupta and Sbragaglia (2016)],volume-tracking method [Rudman (1998)], phase-field method [De Menech (2006)], front-tracking method [Tryggvason, Bunner, Esmaeeli et al. (2001)], fractional volume of fluid (VOF) [Chekifi, Dennai and Khelfaoui (2015)], the level-set method (LSM) [Bjørklund (2009)], and many others. Afkhami et al. [Afkhami, Leshansky and Renardy (2011)] used VOF and "height function" (HF) to simulate droplet breakup in a symmetric microfluidic T-junction. Bedram et al. [Bedram and Moosavi (2012)] used the VOF method to study the generation of droplets in T-junction configuration to generate uniform droplets; their results indicate that the system performance is in its optimum condition at a specific Capillary number (i.e. 0.02). The volume of fluid method is applied to model the shape of a droplet which was driven by an external permanent magnet in a cylindrical computational domain [Afkhami, Renardy, Renardy et al. (2008)]. Hirt et al. [Hirt and Nichols (1981)] presented the VOF techniques for interface capturing using non-uniform mesh. Numerical simulation will be performed in this work to study the droplets dynamics behaviour inside fluidic oscillator.

The fluidic oscillator is a useful tool for flow control applications, many studies have only focused the fluidic oscillator for continuous flow, rather than dispersed flow. In this paper, we use the typical geometry, which includes double T-junction to produce simultaneous

droplets of gasoil on water, the T-junction is connected by the fluidic oscillator. The formation of droplets is computed by volume-of-fluid method (VOF). We have suggested two models of oscillator with two different feedback length (loop) to see its effect on droplets frequency in the output of microsystem. focus the effect of as in a microfluidic system, the effects of inertia and gravity in the volume does not play an important role with respect to the macroscopic scale, we have discussed the effect of surface tension by using of several values between both phases. In this work, the impact of applied pressure on T-junction is also analyzed. Numerical studies are conducted to select droplets passed by both feedback channel, when the jet is switching from attachment wall to another, it leaves the oscillator by output channel which leads a few droplets to leave the oscillator. two-dimensional and time-dependent information such as pressures and velocities that are difficult to measure experimentally, and can thus provide mechanistic insights needed to check various hypotheses.

2 Geometrical characteristics

Geometry we have adopted to model the oscillator for dropletlets is based on the study by Dennai et al. [Dennai, Khelfaoui, Benyoucef et al. (2011)] for the mixture using air as the fluid, the same model has been modified and studied experimentally by Meng et al. [Meng, Xu and Yu (2013)] for oscillation generation using water as the fluid frequency. Then we put in the same geometry with some changes, is chatting in two models, fluidic oscillator with short loop (FOSL) and fluidic oscillator with long loop (FOLL), they are adding a T-junction for producing dropletlets for come to a complete and capable of producing and manipulating dropletlets and adequately represent the phenomena in this experiment model. The 2D model consists mainly of T-junction, two feedback loops and an output, the following two figures show the geometric characteristics and the dimensions of (FOLL).
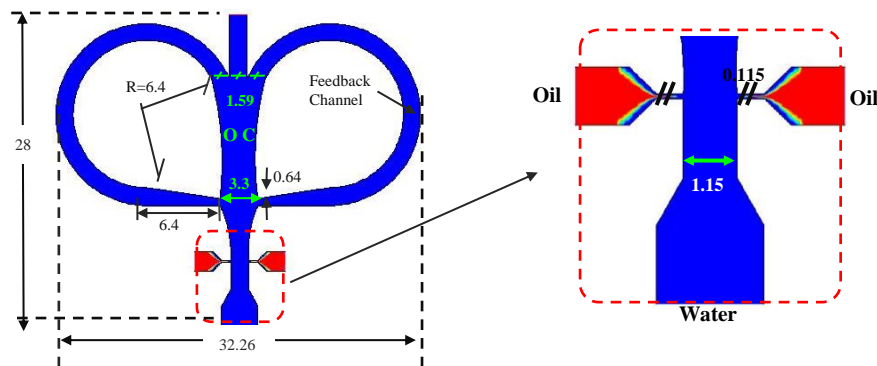
Figure 1: Geometrical characteristic of fluidic oscillator with short loop (FOSL) and long loop (FOLL), The same dimension are kept for both model, except the length that is different of the feedback channel (loop) length, where: $L_{FOLL}=1.5xL_{FOSL}$. OC: oscillation chamber. All dimensions are in (mm).

Fig. 1 presents the geometrical characteristics of the microfluidic oscillators connected by double T-junction. It shows the main parts of the device that include: both inlet of T-

junction, oscillating zone, outputs. Meshing of both geometries was performed using Gambit 2.2.3, we used a structured grid (quadratic cells) with variable density depending on the area (thinner in smaller areas and diameters). The short model has 13750 elements, while the long model has 17550 elements. During the calculation, all parameters will be kept the same, the only different is the feedback channel length, this parameter will be considered for the effect of all comparison of obtained results, in the next section we test our models for the oscillation to identify the efficiency of Coanda effect. In this stage, no droplet is existing in our models,

3 Approximation of the oscillation frequency

For liquids, generally, the oscillation frequency *f*, presented in expression (1), is strongly dependent on the switching time, because the speed of wave propagation is higher than the jet velocity in the nozzle-to-splitter path. Typically, the transmission time for operation with liquids is approximately two or four orders lower than the switching time. For gases, expression (2), the oscillation frequency depends on both the transmission time and the switching time [Yanrong, Someya, Koso et al. (2013)]. It can be identified by the discrete fast Fourier transform method (FFT)

$$\text{fr} = \frac{1}{2\tau_s} \qquad \text{(for liquid)} \tag{1}$$

$$\text{fr} = \frac{1}{2(\tau_t + \tau_s)} \qquad \text{(for gas)} \tag{2}$$

In fluidic oscillators with loops of fluid feedback, the lengths of channels play an important role in determining the oscillation frequency fr [Hz] as well as the operating fluid proprieties, because these devices tend to keep a more or less constant value of Strouhal number [Tesař (2015)]. Traditionally, range of operating frequencies of oscillators is from fr~50 Hz to fr~300 Hz identified with an amplifier with outer size from 20 mm to 200 mm. A higher frequencies could be obtained with the resonator designs up to fr~500 Hz [Tesař, Zhong and Rasheed (2013)]. Because speed of sound in typical applications does not vary, the characteristic property of these oscillators is their constant frequency of oscillation. Nevertheless, the upper limit of frequencies is still below the kilohertz range. Subsequently, to increase the oscillation frequencies requires making the oscillator, a special microfabrication technique would be necessary due to inevitable small size. On the other hand, the small size requires working with smaller flowrates than would be desirable in typical applications.

4 Pulsation test

Computational fluid dynamics software (CFD) was used to investigate the flow field in the microfluidic oscillator, it solves the two-dimensional Reynolds-averaged Navier-Stokes equations in a general curvilinear coordinate system, which provides conservation equations for mass, momentum, and energy. As a first step, the system's boundaries, its subdivisions, the types of interface and the contour faces were performed, commercial software to build and to mesh models for CFD calculations, was used to set up the virtual unit. We have started by defining the plan of two-dimensions (2D) to study the flow

evolution reported in this study, however, for the FOSL, the mesh consists of 13750 quadrilateral cells and 14614 nodes, while for FOLL, the mesh consists of 17550 quadrilateral cells and 18794 nodes. The test of oscillation performance for microfluidic oscillator modeling is assumed with incompressible fluid flow (water). Its density and viscosity respectively are 998.2 kg/m^3 and 0.001 kg/m·s^{-1}, it is assumed that no-slip boundary conditions at all walls. As the flow is axisymmetric the complete geometry is taken into consideration. The calculations were carried out under different values of operating pressure, in the right and the left inlet. For the outlet of both models the pressure Atmospheric is taken in consideration. Additionally, the flow is computed using the laminar solution, with a time step 10^{-5}. The main physical priorities of water taken I calculation are:

- The density: 998 kg·m^{-3}
- The temperature: 300 K.
- The viscosity: $\mu=0.001$ kg/s·m^{-1}
- The important results of water test are shown in the next figure:
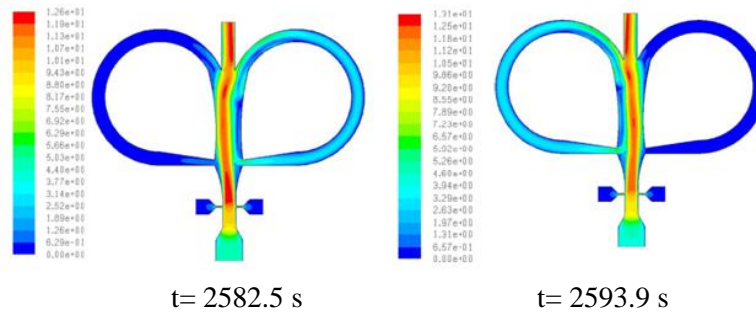
t= 2582.5 s   t= 2593.9 s

Figure 2: Velocity contour in two instants t=2582.5 s and t=2593.9 s.
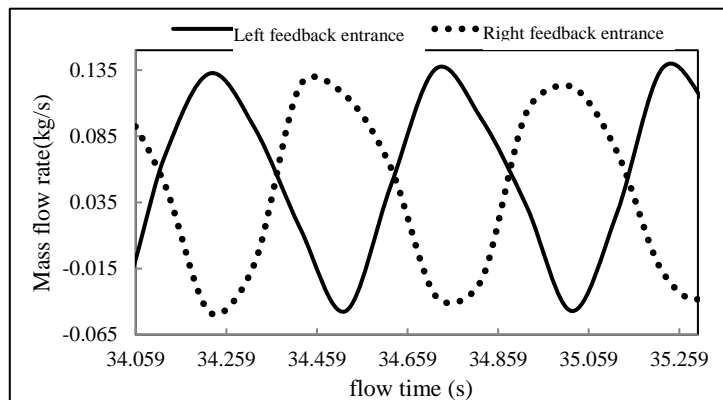
Figure 3: Temporal evolution of the mass flow rate in the entrance of both feedback loops, with the operating pressure 1.5 bar and low inlet=left right=1.4 bar (FOSL case).
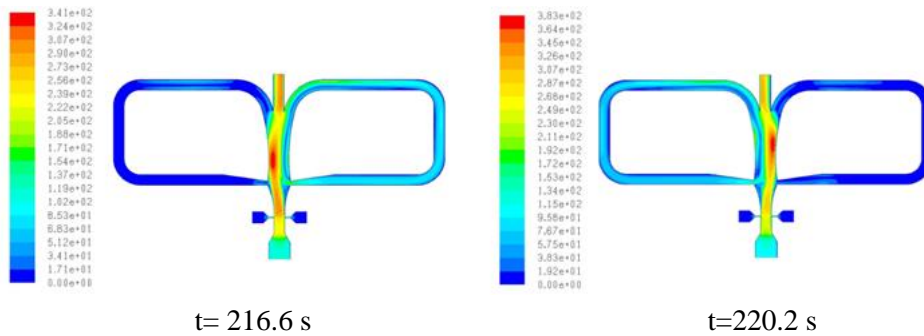
t= 216.6 s   t=220.2 s

Figure 4: Velocity contour in two instants t=216.6 set t=220.2 s
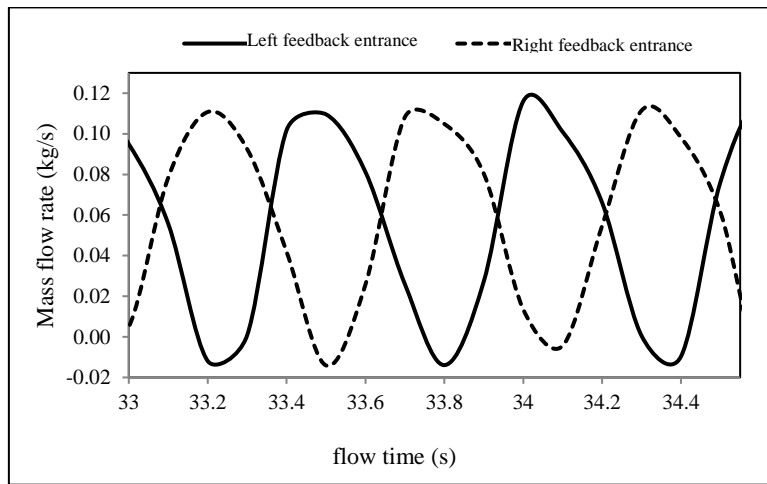
Figure 5: Temporal evolution of the mass flow rate in the entrance of both feedback loops, with the operating pressure 1.5 bar and low inlet=left right=1.4 bar (FOLL case).

In the figures above (2, 3, 4 and 5), we introduced the mass flow in the entrance of both feedback channel of both models short and long, in addition of the velocity contour distribution in the microdevice is presented. The numerical analysis of the mass transfer in both fluidic oscillator models has shown that, the hydrodynamic flow structure had a strong impact on the oscillating mechanism, that is based on the Coanda effect. Fig. 3 and 5 show the evolution of the mass flow rate in the entrance of both loops show a sinusoidal and stable behavior for both models, with the oscillation of the mass flow rate between highest and lowest values, the values of the (FOLL) are lower than those of (FOSL), this difference is due to the length of the loop, we can also observe that the oscillation take small negative values of mass flow rate. which indicates that a low return flow to the chamber oscillation, this return happened during the time of transfer of the loop to the other, this phenomenon is experimentally approved by Yanrong et al. [Yanrong, Someya, Koso et al. (2013)] results, the analysis of velocity contour, using sequencer videos, allows to well observe these vortex development from the down side to the upper zone of the oscillation chamber, a further elongation of the loop effects is clearly observed in the terminals of oscillation, which take an important terminals (-0.01 to 0.11 kg/s) for

(FOLL), while between -0.35 and 0.135 kg/s for FOLL, we assume that this difference is due to the flow time in loops, returns that longer loops in the 2nd models. In which long time of flow inside the loop allows to increase the volume of water in the loop. The results of the hydrodynamic study of both models allowed to identify the best conditions for oscillation, to use these structures for the manipulation of droplets in the following study.

5 Numerical method for droplets calculations

The segregated solver for an unsteady laminar flow was used in CFD, the volume of fluid method was performed to track the interface between the oil droplets and the continuous phase. The VOF model is a surface-tracking technique that is useful when studying the position of the interface between two immiscible fluids. A single set of momentum equations is shared by the fluids, and the volume fraction

of each of the fluids in each computational cell is tracked throughout the domain. The VOF model uses phase averaging to define the amount of continuous and dispersed phase in each cell. A variable, α, was defined as [Anna (2007)]:

$\alpha=1\Longrightarrow$ when the cell is 100% filled with continuous phase

$\alpha=0\Longrightarrow$ when the cell is 100% filled with dispersed phase

$0<\alpha<1\Longrightarrow$ when the cell contains an interface between the two phases.

The density ρ, and viscosity μ, for both phases (water and gasoil) can be calculated using a linear dependence: The subscript 1 is chosen for the continuous liquid (primary) phase, while the subscript 2 for the discrete phase (droplets)

$\rho=\rho_1 \alpha+\rho_2 (1- \alpha)$ (3)

$\mu= \mu_1 \alpha+\mu_2 (1- \alpha)$ (4)

The geometric reconstruction scheme used in this study is based on the work of Youngs (1982) and further described by Rudman [Rudman (1997)]. This scheme permits a piecewise-linear approach, which assumes that the interface has a linear slope within each cell, and the position of the interface is calculated from the volume fraction and its derivatives in the cell. The solutions of the velocity field and pressure are calculated using a body-force-weighted discretization scheme for the pressure and the Pressure-Implicit with Splitting of Operators (PISO) scheme for the pressure velocity. The CFD software was used to simulate the flow of oil droplets into a fluidic oscillator. it uses a control-volume-based technique to convert the governing equations into algebraic equations that can then be solved numerically. The governing equations are the mass conservation equation for each phase and the momentum equation:

$\partial_t c +\vec{u}\nabla c = 0$ (5)

where the velocity is given by u. In addition, a single momentum equation is used for the mixture of two-phase-fluid. The momentum equation hence is described by:

$\frac{\partial}{\partial t}(\rho\vec{u}) + \nabla.(\rho\vec{u}\vec{u}) + \nabla\vec{u}.\nabla[\mu] = -\nabla P - F$ (6)

Where F is the surface tension force $F = \sigma\kappa (x)n,$ κ is the curvature of the interface and n is a unit vector normal to the interface. σ is the surface tension coefficient. Flow regimes are taken to be two-dimensional laminar. The density and viscosity of the fluid is assumed

to be constant for each phase. In these models, the influence of the interfacial tension and the operating pressure are focused. With the boundary conditions for no-slip at the wall assembly. The PISO scheme is considered diagram pressure-velocity coupling, while PRESTO! is taken as the pressure discretization scheme. The geometric pattern of the reconstruction is used for interpolation of the geometry of the interface. These results are discussed in the following section. However, the intervals mesh sizes we used for the first model is *h=0.008 mm*, while *h=0.012 mm* for the second model. A grid independence study has been checked by varying the number of cells in the domain. A grid having 14614 cells for *h=0.008 mm* was sufficient as increasing of refinement didn't produce any change in fluid flow oscillation in term of frequencies and stability, at the output of oscillator. The requirement to successfully conduct droplets led us to a very large number of grid cells, where the type of structured mesh was used. 14614 grid points have been required to achieve a converged solution. Velocities corresponding to a low Capillary number ($Ca<0.01$) are used in the simulation.

6 Validation test of VOF method

In last decades droplet simulation was widely studied using CFD codes, such as LBM, VOF, Level set method and others. In this subsection the volume of fluid method is verified for droplet formation and compared to previous available works, we compare a published paper of drop let breakup by cross junction, the paper has been accepted for publication.

Table 1: Droplets generation and comparison with numerical and experimental work

Authors	Geometry size	fluids	(μ_d/μ_c)	(Q_d/Q_c)	Droplet diameter
Shi et al. [Shi, Tang and Xia (2014)] (LBM method)	$W_o=W_w=20$ μm $W_d=12$ μm (80×340 μm)	Water in oil	0.25	0.11 0.3 0.5	70 μm 95.8 μm 155 μm
Wu et al. [Wu, Luo, Liu et al. (2015)] (VOF method)	$W_o=W_w=184$ μm $W_d=400$ μm	Water in oil	0.02	0.05 0.1 0.2	49.5 μm 63.8 μm 84 μm
Our model (VOF method)	$W_o=W_w=1$ mm $W_d=0.8$ mm (4×7 mm)	Water in oil	0.33	0.1 0.14 0.2	0.3 mm 0.4 mm 0.61 mm

Significant numerical and experimental data are existing in the literature for the droplet formation, the same fluids (water and oil) are used in this test, while the geometry dimension, the viscosity ratio and flow rate ratio are different which is normal to check a qualitative comparison and validation. a comparison of droplet flow pattern with Shi et al. [Shi, Tang and Xia (2014)] shows a good agreement in term of droplet diameter. In addition, increasing of flow rate ratio leads to increasing of droplet diameter. The model was also validated by comparing the simulation results against a wide range of experimental results in the form of the sequential photographs presented by Shi et al. [Shi,

Tang, Xia et al. (2014)] and [Gupta and Sbragaglia (2016)]. From the above comparisons and analysis, all the qualitative and quantitative numerical results are in good agreement with VOF method results. Therefore, the methodology in the present numerical study is reliable and efficient for the research of droplet flow inside fluidic oscillator with various dimensions. Therefore, further investigations can be carried out based on the method.

7 Results analysis and discussion

In order to better understand the phenomena that occur during the study. We summarize the most important results in the following figures:
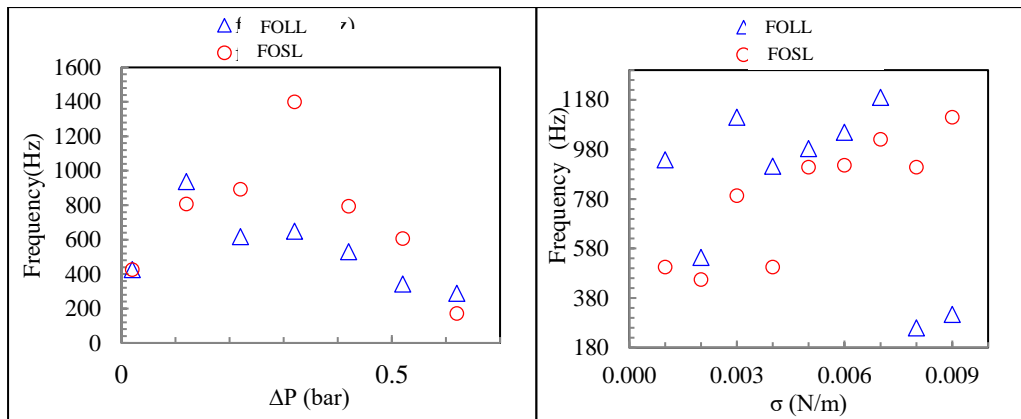
Figure 6: Frequency of droplets at the output of both oscillators as function of ΔP and surface tension.
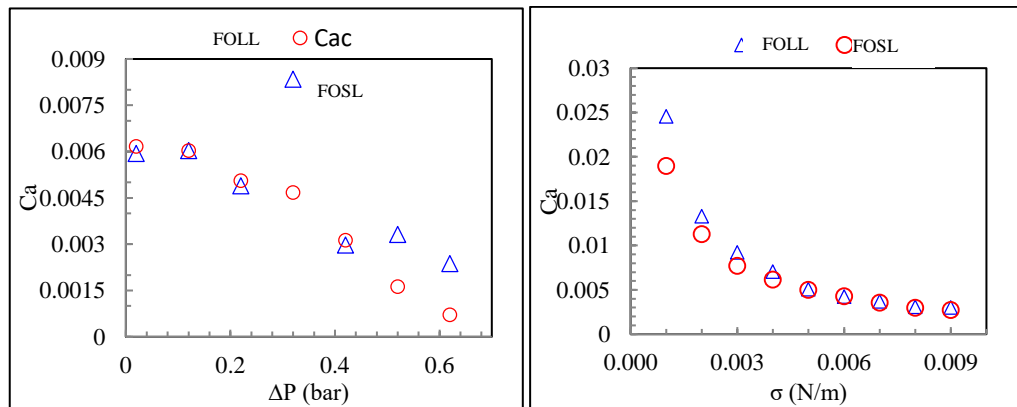
Figure 7: Evolution of capillary number (Ca) as function of difference of pressure and surface tension for both oscillator.

The Fig. 6 shows the frequency evolution as function of the difference applied pressure and the surface tension. The mechanism of droplet formation is effected by a phase shearing another. This causes a shear deformation of the interface may or may not lead to the rupture of a drop [Bazhlekov, Anderson and Meijer (2006)]. The shear in the interface depends primarily on the operating pressure on both phases, indeed, the pressure

influences the flow of the droplets in the fluidic oscillator. On the other hand, the Coanda effect leads jet stream to oscillate from one attachments wall to the other one, this process makes the jet flows into the feedback channels. As a result, droplets also are pulsating from one feedback channel to the other one, during this cycle, merging of a few droplets is occurred while oscillating in the oscillation chamber at low surface tension. In the Fig. 6 we have also presented the frequency as function of the interfacial tension between, the latter is very important parameter in the multiphase flow, it plays an important rule regarding droplets shape, stability, and dispersion. Surface tension allows to describe the attraction between molecules of both fluids, it can also reflects the rigidity of fluid. this parameter is very necessary for droplets dynamic characteristics in small scale devices. In the Fig. 6 we can see that the droplets frequency variation in the output of both microsystem depending on surface tension between both phases, in which the frequency is increasing by increasing of surface tension, which leads the molecules in both phases to be so attracted, this make them to flow with high dispersion. As a result, the fusion the droplets flow with rare fusion and make high frequency.
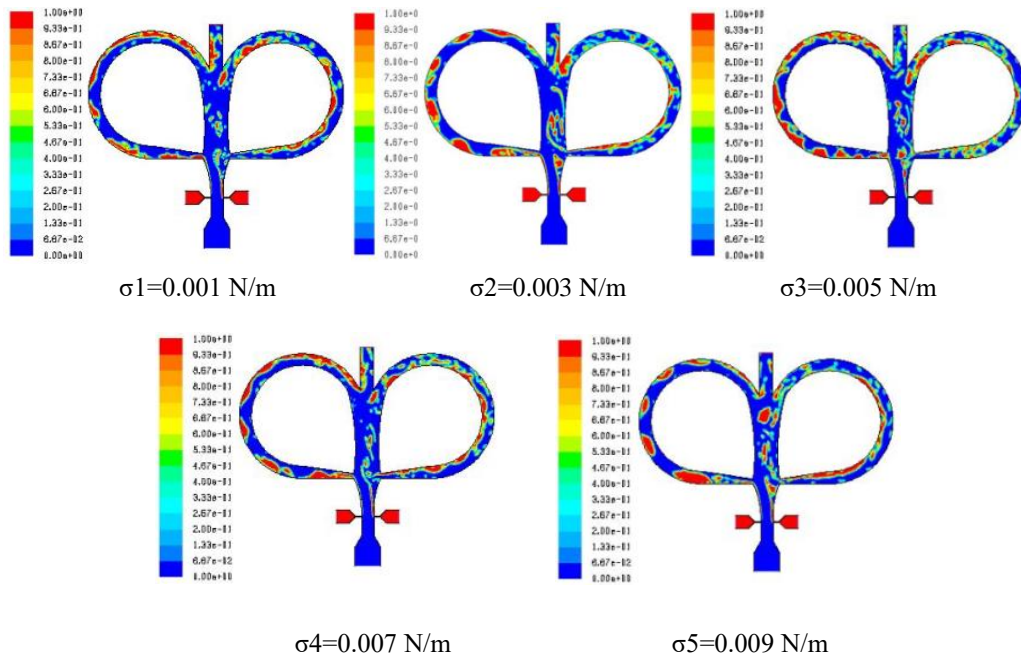

σ1=0.001 N/m   σ2=0.003 N/m   σ3=0.005 N/m

σ4=0.007 N/m   σ5=0.009 N/m

Figure 8: Sequence image of droplets distribution for every surface tension values in the oscillator (FOSL). Δp=0.02 bar. (P_{low}=1.9 and P_{righ}=P_{left}=1.88 bar)

In Fig. 7, the capillary number Ca evolution is presented for both parameters Δp and σ, the Capillary numbers simulated, At exceedingly low capillary numbers (Ca<0.01), viscous effects are dominated by interfacial stress, the droplet breakup can occur because of a pressure gradient squeezing against the immiscible interface stabilized by the confined geometry [Ong, Hua, Zhang et al. (2007)].

In the FOSL model of the above figures, the volume fraction of both phases in the entrance of two loops feedback channels is described. We use the oscillatory frequency obtained

and identified by the discrete fast Fourier trans form method (FFT). We assume that the applied pressure became low efficient in the long loop, which leads to have low frequency, this case is required for several application, such as mixing application during the flow of droplets, the latter contain chemical reactors and need a different residence time to have a reaction, also it is clearly observed that the frequency development takes form in both models (1400 Hz for SLOF and 910 Hz for FOLL), then the frequency tends to decrease due to the accumulation of droplets in the feedback channel especially for the FOLL, thus, the growing of droplets with low velocity inside the oscillation zone leads to fusion to be occurred which make a thread flow regime to be formed. Furthermore, the droplets take long time in the loop feedback channel of FOLL relative to the FOSL. Consequently, the droplets frequency at the output of microsystem is higher. The Fig. 8 shows both phases distribution in the FOSL model for $\Delta p=0.02$ bar. ($P_{low}=1.9$ and $P_{righ}=P_{left}=1.88$ bar), it also monitors and provides us how the droplets are flowing as function of five surface tension values, it is clearly observed that the biggest one ($\sigma5=0.009$ N/m) monitors the most dispersed droplets. Which affirm our analysis above, as surface tension is smaller ($\sigma1=0.001$ N/m), droplets are lost their uniform shape and accumulates at the upper side of the oscillation zone, which makes a long stream flow at the entrance of feedback channel, due to the merging of consecutives droplets.

8 Conclusion

Droplets flow-manipulation by fluidic oscillators was numerically studied; two models was proposed, in order to investigate the droplets dynamics and frequencies inside fluidic devices, geometrically, the same dimensions were kept for both fluidic oscillator, the only different is the feedback channel length (the long one is FOLL and the short one is FOSL). The simulation of dispersed phase systems with several of droplets requires the use of simplified models. Therefore, the VOF model is used in this work, our approach is suited for simulating two dimensional problems in which no large topological changes occur. The numerical simulations showed that the fluidic oscillator may be used to manipulate, separate and select droplets. We have studied the influence of operating pressure on the fluidic oscillator on the droplets flow and its effect on the frequency, where we have found that the increase of difference of the applied pressure causes an increase of maximal frequency of droplets until a top. Additionally, we have found that the interfacial tension affects on droplets dispersion and its frequency, where the increase of this parameter makes more coherent and flow with high dispersion, thus the droplets frequency was high for high surface tension. The precedents parameters were studied in accompany with the loop channel length, where the latter was played an important role in the droplets frequency, the droplets take long time in the loop feedback channel of FOLL relative to the FOSL which effect directly on the droplets frequency. On the basis of the obtained results, we can use the proposed fluidic oscillator models in the manipulation of droplets without moving part. Further investigations of different fluid and the use of fluidic oscillator in biochemical application will be experimentally done. Besides, if the main drop was carried a chemical or biochemical sample, in this case multidisciplinary simulation will be required.

References

Timgren, A.; Trägårdh, G.; Trägårdh, C. (2007): CFD Modelling of Drop Formation in a Liquid-Liquid System. *6th International Conference on Multiphase Flow*, ICMF.

Afkhami, S.; Leshansky, A.; Renardy, Y. (2011): Numerical investigation of elongated drops in a microfluidic T-junction. *Physics of Fluids*, vol. 23, no. 2, pp. 022002.

Afkhami, S.; Renardy, Y.; Renardy, M.; Riffle, J.; St Pierre, T. (2008): Field-induced motion of ferrofluid droplets through immiscible viscous media. *Journal of Fluid Mechanics*, vol. 610, pp. 363-380.

Bjørklund, E. (2009): The level-set method applied to droplet dynamics in the presence of an electric field. *Computers & Fluids*, vol. 38, no. 2, pp. 358-369.

Bazhlekov, I. B.; Anderson, P. D.; Meijer, H. E. (2006): Numerical investigation of the effect of insoluble surfactants on drop deformation and breakup in simple shear flow. *Journal of colloid and interface science*, vol. 298, no.1, pp. 369-394.

Bedram, A.; Moosavi, A. (2012): Numerical investigation of droplets breakup in a microfluidic T-junction. *Applied Mechanics and Materials*, Trans Tech Publ.

Bobusch, B. C.; Woszidlo, R.; Bergada, J. M.; Nayeri, C. N.; Paschereit, C. O. (2013): Experimental study of the internal flow structures inside a fluidic oscillator. *Experiments in Fluids*, vol. 54.

Chekifi, T.; Dennai, B.; Khelfaoui, R. (2015): Numerical Simulation of Droplet Breakup, Splitting and Sorting in a Microfluidic Device. *Fluid Dynamics & Materials Processing*, vol. 11, no.3, pp. 205-220.

Davies, R. C. (1970): Functional characteristics of fluid elements. *Fluidics Quarterly*, vol. 2, no. 2, pp. 1-43.

De Menech, M. (2006): Modeling of droplet breakup in a microfluidic T-shaped junction with a phase-field model. *Physical Review E,* vol. 73, no. 3, pp. 031505.

Dennai, B.; Khelfaoui, R.; Benyoucef, B. et al. (2011): Passive Micromixing Solution. *Sensors & Transducers,* vol. 131, no. 8, pp. 121.

Gregory, J. W.; Sullivan, J. P.; Raman, G.; Raghu, S. (2007): Characterization of the microfluidic oscillator. *AIAA Journal,* vol. 45, no. 3, pp. 568-576.

Gupta, A.; Sbragaglia M. (2016): A lattice Boltzmann study of the effects of viscoelasticity on droplet formation in microfluidic cross-junctions. *The European Physical Journal E, Soft Matter,* vol. 39, no. 1, pp. 2.

Gregory, J.; Tomac, M. N. (2013): A review of fluidic oscillator development. *Aiaa Fluid Dynamics Conference*, vol. 37, pp. 151-168.

Huichun, Z.; Gary, D.; Jiaqiang, Z. (2012): Wind tunnel experiment of influence on droplet size distribution of flat fan nozzles. *Transactions of the Chinese Society for Agricultural Machinery,* vol. 43, no. 6, pp. 53-57.

Hirt, C. W.; Nichols B. D. (1981): Volume of fluid (VOF) method for the dynamics of free boundaries. *Journal of computational physics,* vol. 39, no. 1, pp. 201-225.

Jebrail, M. J.; Bartsch, M. S.; Patel, K. D. (2012): Digital microfluidics: a versatile tool for applications in chemistry, biology and medicine. *Lab on a Chip,* vol. 12, no. 14, pp. 2452-2463.

Kobayashi, I.; Vladisavljević, G. T.; Uemura, K.; Nakajima, M. (2011): CFD analysis of microchannel emulsification: Droplet generation process and size effect of asymmetric straight flow-through microchannels. *Chemical Engineering Science*, vol. 66, no. 22, pp. 5556-5565.

Lakebrink, M. T.; Mani, M.; Winkler, C. (2017): *Numerical investigation of fluidic oscillator flow control in an s-duct diffuser.* Aiaa Aerospace Sciences Meeting

MDS-Ocata, D. F. Ÿ. (2000): A revolution in biological and medical sciences. *Analytical Chemistry*.

Meng, X.; Xu, C.; Yu, H. (2013): Feedback fluidic flowmeters with curved attachment walls. *Flow Measurement and Instrumentation*, vol. 30, pp. 154-159.

Ong, W. L.; Hua, J.; Zhang, B.; Teo, T. Y.; Zhuo, J.; Nguyen, N. T. et al. (2007): Experimental and computational analysis of droplet formation in a high-performance flow-focusing geometry. *Sensors and Actuators A: Physical,* vol. 138, no. 1, pp. 203-212.

Renaudin, A.; Tabourier, P.; Zhang, V. (2006): SAW nanopump for handling droplets in view of biological applications. *Sensors and Actuators B: Chemical,* vol. 113, no. 1, pp. 389-397.

Rudman, M. (1997): Volume-Tracking methods for interfacial flow calculations. *International Journal for Numerical Methods in Fluids,* vol. 24, pp. 671-691.

Rudman, M. (1998): A volume-tracking method for incompressible multifluid flows with large density variations. *International Journal for numerical methods in fluids,* vol. 28, no. 2, pp. 357-378.

Shakouchi, T. (1989): A new fluidic oscillator, flowmeter, without control port and feedback loop. *Journal of Dynamic Systems, Measurement, and Control*, vol. 111, no. 3, pp. 535-539.

Sarrazin, F.; Bonometti, T.; Prat, L.; Gourdon, C.; Magnaudet, J. (2007): Hydrodynamic structures of droplets engineered in rectangular micro-channels. *Microfluidics and Nanofluidics*, vol. 5, no. 1, pp. 131-137.

Simões, E. W.; Furlan, R.; Bruzetti Leminski, R. E.; Pereira, M. T.; Morimoto, N. I. (2005): Microfluidic oscillator for gas flow control and measurement. *Flow Measurement and Instrumentation*, vol. 16, no. 1, pp. 7-12.

Shah, G. J.; Ohta, A. T.; Chiou, E. P. Y.; Wu, M. C.; Kim, C. J. (2009): EWOD-driven droplet microfluidic device integrated with optoelectronic tweezers as an automated platform for cellular isolation and analysis. *Lab on a Chip,* vol. 9, no. 12, pp. 1732-1739.

Seto, W.; Tsang, D.; Yung, R.; Ching, T. Y.; Ng, T. K. et al. (2003): Effectiveness of precautions against droplets and contact in prevention of nosocomial transmission of severe acute respiratory syndrome (SARS). *The Lancet*, vol. 361, no. 9368, pp. 1519-1520.

Shi, Y.; Tang, G. H.; Xia, H. H. (2014): Lattice Boltzmann simulation of droplet formation in T-junction and flow focusing devices. *Computers & Fluids,* vol. 90, pp. 155-163.

Tesař, V. (2015): High-frequency fluidic oscillator. *Sensors and Actuators A: Physical,* vol. 234, pp. 158-167.

Tryggvason, G.; Bunner, B.; Esmaeeli, A.; Juric, D.; Al-Rawahi, N. et al. (2001): A front-tracking method for the computations of multiphase flow. *Journal of Computational Physics*, vol. 169, no. 2, pp. 708-759.

Thiele, C.; Spandl, J. (2008): Cell biology of lipid droplets. *Current opinion in cell biology*, vol. 20, no. 4, pp. 378-385.

Tesař, V.; Zhong, S.; Rasheed, F. (2013): New Fluidic-Oscillator Concept for Flow-Separation Control. *AIAA Journal,* vol. 51, no. 2, pp. 397-405.

Wu, P.; Luo, Z.; Liu, Z.; Li, Z.; Chen, C. et al. (2015): Drag-induced breakup mechanism for droplet generation in dripping within flow focusing microfluidics. *Chinese Journal of Chemical Engineering,* vol. 23, no. 1, pp. 7-14.

Yang, J. T.; Chen, C. K.; Tsai, K. J.; Lin, W. Z.; Sheen, H. J. (2007): A novel fluidic oscillator incorporating step-shaped attachment walls. *Sensors and Actuators A: Physical*, vol. 135, no. 2, pp. 476-483.

Yan, Y.; D. Guo; Wen, S. Z. (2012): Numerical simulation of junction point pressure during droplet formation in a microfluidic T-junction. *Chemical Engineering Science*, vol. 84, pp. 591-601.

Yoon, S.; Kim, J. A.; Lee, S. H.; Kim, M.; Park, T. H. (2013): Droplet-based microfluidic system to form and separate multicellular spheroids using magnetic nanoparticles. *Lab Chip*, vol. 13, no. 8, pp. 1522-1528.

Yanrong, L.; Someya, S.; Koso, T.; Aramaki, S.; Okamoto, K. (2013): Characterization of periodic flow structure in a small-scale feedback fluidic oscillator under low-Reynolds-number water flow. *Flow Measurement and Instrumentation*, vol. 33, pp. 179-187.